Graded multidimensional clinico-radiological variations in Alzheimer's disease and posterior cortical atrophy

Running head: Graded phenotypes in Alzheimer's disease

Ruth U. Ingram PhD[1*], Dilek Ocal PhD[2*], Ajay D. Halai PhD [3], Gorana Pobric PhD [1], David Cash[2], Sebastian J. Crutch PhD [2], Keir X.X. Yong PhD [2†] & Matthew A. Lambon Ralph PhD [3†]

[1]Division of Psychology and Mental Health, School of Health Sciences, University of Manchester, UK
[2]Dementia Research Centre, UCL Institute of Neurology, London, UK
[3]MRC Cognition & Brain Sciences Unit, University of Cambridge, UK
*Joint first authors
†Joint senior authors

Corresponding authors
Ruth U. Ingram, PhD
University of Manchester, Manchester, M13 9PL
Email: ruth.ingram@manchester.ac.uk

Prof. Matthew A. Lambon Ralph,
MRC Cognition & Brain Sciences Unit, University of Cambridge, UK
Email: matt.lambon-ralph@mrc-cbu.cam.ac.uk
Tel: +441223 767754

ORCiD:
Ingram: 0000-0003-0245-3030
Ocal:
Halai: 0000-0003-1725-7948
Pobric: 0000-0002-8655-9571
Cash:
Crutch: 0000-0002-4160-0139
Yong: 0000-0002-9708-3599
Lambon Ralph: 0000-0001-5907-2488
Open access: For the purpose of open access, the UKRI-funded authors have applied a Creative Commons Attribution (CC BY) licence to any Author Accepted Manuscript version arising from this submission.

Abstract

Alzheimer's disease spans a heterogeneous collection of typical and atypical phenotypes. Posterior cortical atrophy represents one of the most striking examples, characterised by prominent impairment in visual and other posterior functions in contrast to typical, predominantly amnestic Alzheimer's disease. Whilst proposed posterior cortical atrophy subtypes include dorsal, ventral, caudal and dominant parietal presentations, investigations of posterior cortical atrophy subtypes are rare. **Objective**: The current study establishes how the similarities and differences of cognition and neural integrity within posterior cortical atrophy and typical Alzheimer's disease (and by extension other Alzheimer's disease variants), can be conceptualised as systematic variations across a unified transdiagnostic, graded multidimensional space. **Methods**: Principal component analysis was applied to detailed neuropsychological cognitive and visual data from a large cohort of posterior cortical atrophy (N=93) and typical Alzheimer's disease patients (N=58). Voxel-based morphometry was then used to explore neural correlates of the emergent transdiagnostic PCA phenotype dimensions. **Results**: The principal component analysis for posterior cortical atrophy extracted three dimensions, reflecting general cognitive impairment, visuoperceptual deficits and visuospatial impairments. Projecting typical Alzheimer's disease cases into the posterior cortical atrophy-derived multidimensional space, and vice versa, revealed graded, overlapping variations between cases along these dimensions, with no evidence for categorical-like clustering of the patients. Likewise, the relationship between neural integrity and scores on the extracted dimensions was overlapping for PCA and tAD. **Interpretation**: The results are consistent with phenotypic continua spanning posterior cortical atrophy and typical Alzheimer's disease, arising from systematic graded variations within a transdiagnostic, multidimensional neurocognitive geometry.

Introduction

Alzheimer's disease (AD) generates heterogeneous typical (amnestic) and atypical phenotypes [1, 2], including visual, logopenic, behavioural and dysexecutive presentations [3]. However, these categorical classifications do not fully capture the graded variation within and between variants, or mixed phenotypes [2, 4-6]. This challenges: diagnosing AD variants; selecting appropriate therapeutics and rehabilitation pathways; and research recruitment [4, 7]. Utilising detailed neuropsychological and neuroimaging data from 93 posterior cortical atrophy (PCA) and 58 typical AD (tAD) patients, the current study established and mapped the graded neuropsychological and neuroimaging dimensions that underpin the patient variations. The resultant transdiagnostic, multidimensional neurocognitive geometry captures the variations within and between PCA and tAD subtypes.

Phenotypic variation within and between tAD and PCA ("visual-spatial AD" [7]) illustrates these challenges. PCA symptoms include space and object perception deficits, constructional apraxia, environmental agnosia and alexia [6, 8, 9]. PCA is variously conceptualised as a discrete nosological entity [10], an atypical variant of AD [11], or an extreme point in an AD phenotypic continuum [12]. Some comparative studies have shown PCA and tAD differ in key cognitive and visual domains (e.g., delayed auditory/verbal memory worse in tAD), but not significantly in others (e.g., working memory, language, ideomotor praxis) [13]. This highlights the overlapping cognitive variation, which may be missed in studies that employ categorical classification systems to define groups [14, 17]. Furthermore, in tAD, impairments in atypical (non-amnestic) domains including visuospatial processing have been found [2, 12, 18]. Accordingly, the overlapping presentations of AD could be conceptualised as graded phenotypic spectra, which would be consistent with growing evidence that AD heterogeneity could be due to the spreading pattern of tau along functional brain networks [19-24]. This study therefore employed an approach which: (1) situates participants with tAD and PCA in the same graded multidimensional space, to capture the patterns of overlapping and/or non-overlapping cognitive performance, and then (2) relates the transdiagnostic phenotype dimensions to the pattern of atrophy across the whole brain, to understand how shared cognitive variation may reflect common atrophy patterns.

Traditional categorical classification systems fail to account for these heterogenous clinical presentations and potential phenotypic spectra. Reconceptualising variants/subtypes as subregions with fuzzy boundaries within a graded multidimensional space offers an alternative approach [2, 12, 14, 16], which has been successfully applied to post-stroke aphasia [29, 30], primary progressive aphasia [31], semantic dementia [32], fronto-temporal lobar degeneration [33] and logopenic progressive aphasia [34]. The current study employed a similar approach to explore both cognitive and neuroanatomical variation within and between PCA and tAD. This was achieved through the application of principal component analysis to a large-scale, detailed neuropsychological database followed by grey matter voxel-based morphometry, allowing a data-driven exploration of (a) the presence and cognitive nature of phenotypic continua in each

group; and (b) the extent of intragroup and intergroup graded variation in cognition and grey matter volume in the multidimensional space defined by these dimensions.

Methods

Patients

Ninety-three people with posterior cortical atrophy (PCA) were recruited from the Specialist Cognitive Disorders Clinic at the National Hospital for Neurology and Neurosurgery, London, UK. All PCA patients met consensus criteria for PCA-pure [6], and Tang-Wai *et al*. [9] and Mendez *et al*. [8] clinical criteria based on available information at baseline and expert retrospective clinical review. PCA patients with evidence of non-Alzheimer's disease dementia (e.g., dementia with Lewy bodies, or cortico-basal degeneration) in clinical assessment and investigations were excluded.

Fifty-eight people with typical Alzheimer's disease were recruited from the same Specialist Cognitive Disorders Clinic on the basis of meeting the National Institute of Neurological and Communicative Disorders and Stroke and the Alzheimer's Disease and Related Disorders Association (NINCDS-ADRDA) criteria for probable AD with recently proposed revisions [35].

All available molecular or pathological evidence (34 PCA; 39 tAD) supported underlying Alzheimer's disease pathology (63 had a CSF profile compatible with Alzheimer's disease [36, 37]), 3 had positive amyloid PET scans; 10 had autopsy-proven Alzheimer's disease. Patients with biomarker evidence of Alzheimer's disease pathology met the McKhann *et al.* [38] IWG-2 criteria for probable Alzheimer's disease with high biomarker probability of Alzheimer's disease aetiology [39].

The posterior cortical atrophy and typical Alzheimer's disease cases have been included in previous publications [15, 16, 28, 40-44]. All patients provided informed consent under approval from NRES Committee London, Queen Square. Demographic details are summarised in Table 1. There were no significant differences between tAD and PCA groups in either age ($t_{(137)} = .569$, $p = .571$) or symptom duration ($t_{(115)} = 1.907$, $p = .059$). There were more females than males in the PCA group, and more males than females in the tAD group ($\chi^2_{(1)} = 9.35$, $p = .002$). MMSE [45] scores were not significantly different between tAD and PCA ($t_{(141)} = -1.73$, $p = .085$).

Table 1 – Demographic details for each diagnostic group. Age at onset, symptom duration and MMSE score are presented as mean (SD).

Diagnosis	Total N (F)	Age (years)	Symptom duration (years)	MMSE
tAD	58 (22)	57.1 (6.4)	6.2 (3.0)	19.7 (4.9)
PCA	93 (59)	59.9 (8.1)	5.2 (2.6)	21.2 (5.1)

Neuropsychological assessments

Both groups completed the same neuropsychological battery, thus allowing direct comparisons. The tests included in the principal component analysis are shown in **Error! Reference source not found.** and most a re described in Lehmann *et al.* [28], with the addition of letter "A" Cancellation [46], recognition memory for faces [47], and tests of early visual processing. The latter included: hue discrimination (CORVIST [48]), shape discrimination [49], figure/ground separation (VOSP – Visual Object and Space Perception battery [50]), and crowding. Assessments measuring time to complete or number of errors, where a lower value indicates less impaired performance, were inverted so that lower values across all tests indicated worse performance.

Cognitive analysis

All raw cognitive scores were converted to percentages. For time-based measures without a fixed maximum score (letter 'A' cancellation (time); Crowding (time); VOSP dot count (time)), scores were converted to a percentage of the maximum time taken within each cohort. The adequacy of the sample size for each principal component analysis was determined using the Kaiser-Meyer-Olkin measure of sampling adequacy and Bartlett's test of sphericity.

Imputation and component selection

To retain as much information (patients and tests) as possible, missing data were imputed using probabilistic principal component analysis (PPCA) [51], which was also used to select the optimal number of components for subsequent principal component analysis using the imputed dataset (as described in Ingram *et al.* [31]). In this procedure, the number of components for PPCA to extract must be pre-specified. A k-fold cross validation approach was used to choose the component-solution (i.e., number of components) with the lowest root mean squared error (RMSE) for held-out cases over 1000 permutations [52]. The subsequent principal component analyses were also run on a version of the dataset with missing data more strictly removed (no test having more than 12% missing data and no participant having more than 18% missing data) and the factors in the resultant solutions were correlated all above 0.94 with the corresponding components from the solutions reported below.

Principal component analysis

We applied separate principal component analyses to the tAD and PCA cohorts to establish the multidimensional space of each presentation independently (this avoids the possible danger of creating false overlaps by fusing the two groups into an unrepresentative single homogenous space). We applied varimax rotation in order to promote cognitive interpretation of the emergent dimensions (as well as comparisons across the two multidimensional spaces). Normalised factor scores were obtained for each patient, for subsequent neuroimaging analyses and creation of the scatterplots.

Having established the multidimensional spaces for tAD and PCA independently, in order to evaluate the degree and nature of any overlap between the two groups we explored whether there were any regions of

this multidimensional space which would also be occupied by the other group. This was achieved by projecting the neuropsychological scores from one group through the coefficient matrix of the other group (as both cohorts underwent the same cognitive test battery). The results obtained by projecting PCA patients into the tAD-derived multidimensional space are presented in the supplement. Finally, we calculated Pearson correlation coefficients between scores on all extracted factors and (a) age, (b) symptom duration, and (c) MMSE scores to explore the relationship with disease severity (correcting for multiple comparisons).

Image Acquisition

T1-weighted volumetric MR scans were acquired for 71 healthy controls, 70 PCA patients and 14 tAD patients over a 10-year period from 2005 – 2015. Seven PCA and 5 tAD scans were excluded after image quality assurance due to motion and ghosting artifacts, yielding a total number of 71 healthy control, 62 PCA and 9 tAD scans that were included in the final analyses. The majority of scans (controls: 39; PCA: 43; tAD: 8) were acquired on a Siemens Prisma 3T scanner using a magnetisation prepared rapid acquisition gradient echo sequence (MPRAGE) with a 256x256 acquisition matrix, 282mm field of view and the following acquisition parameters: TE=2.9ms, TR=2200ms and TI=900ms. The remaining images (controls: 32; PCA: 19; tAD: 1) were acquired on a 1.5T Sigma MRI scanner using a spoiled gradient echo (SPGR) sequence with a 256x256 image matrix, a 240mm field of view and the following acquisition parameters: TE=6.3ms; TR=14.2ms and TI=650ms.

Image Pre-processing

Image pre-processing involved the following steps: (1) image format conversion from DICOM to NIFTI; (2) tissue segmentation using SPM's unified model [53] (3) the creation of a study-specific grey matter (GM) segment template using SHOOT; (4) normalisation of the segments to the study specific template that generally matches standard space (MNI) in orientation using SHOOT transformations; (5) modulation to account for local volume changes; and (6) smoothing using a 6 mm full-width at half- maximum Gaussian kernel to compensate for inaccuracies in spatial alignment and between-subject differences in anatomy. The smoothed, normalised and modulated SHOOT-imported GM segments were then used for analysis. Image pre-processing steps (3)-(6) were performed for the different analyses (PCA-only and Combined) separately to ensure that the GM segment template only included analysis-specific participant scans.

Voxel-based morphometry

We used whole-brain voxel-based morphometry (VBM) to explore the neuroanatomical substrates (brain atrophy) of the graded variation in cognitive performance in PCA and tAD. VBM analysis was performed using Statistical Non-Parametric mapping (SnPM - [54] – a toolbox within Statistical Parametric Mapping software (SPM12.1 - [55] which allows for pseudo t-statistic images to be assessed for significance using a standard non-parametric multiple comparisons procedure based on permutation testing. Prior to performing the analyses, a whole-brain GM mask was defined to include only voxels for which the

intensity was at least 0.2 in at least 80% of the images to circumvent exclusion of voxels most vulnerable to brain atrophy [56].

Correlations Between Grey Matter Volume and Principal Component-Derived Factor Scores

Two VBM regression analyses were performed using factor scores from the PCA-derived multidimensional space, a PCA-only (N=63) and a PCA/tAD combined (N=71) analysis to explore PCA-specific and shared PCA/tAD associations between GM volume and neuropsychological deficits, respectively. Prior to the PCA/tAD combined analysis tAD patients were projected through the PCA-derived coefficient matrix to situate the tAD and PCA cases within the same multidimensional space (as above). Both regression models included smoothed, modulated, and warped GM volume as the dependent variable, the three principal component-generated factor scores as the independent variables, and age at assessment (mean-centred), total intracranial volume (mean-centred) [57], gender and scanner (3T or 1.5T) as covariates. The PCA/tAD combined analysis included group as an additional covariate. A tAD-only analysis (i.e., relating GM volume to factor scores from the tAD-derived multidimensional space with projected scores for PCA cases) was not performed due to the limited number of available tAD scans.

Statistical significance was determined by permutation testing (10,000 permutations) based on peak-voxel inference and set at $p<.05$ (family-wise error corrected). Scatterplots were created to visualise the relationship between GM volume and factor scores.

Grey Matter Volume Changes in Posterior Cortical Atrophy and Typical Alzheimer's Disease

To aid interpretation of correlation analyses, we assessed differences in voxel-wise GM volume in PCA and tAD relative to healthy controls separately using independent t-tests. Age at assessment (mean-centred), total intracranial volume (mean-centered), gender, and scanner (3T or 1.5T) were included as covariates. Effect size maps are presented in Supplementary Materials.

Results

Scores on all neuropsychological tests for tAD and PCA participants are summarised in Table 2.

Table 2 - Neuropsychology test scores and missing data. Neuropsychology test scores shown as percentage of maximum score per group (higher percentage corresponds to less impairment (less errors, faster time to complete). Missing data is shown as percentage missing per group. Significant differences between diagnostic groups on each test assessed through one-way ANOVA; * Welch's W statistic reported due to heterogeneity of variance. Abbreviations: SD – standard deviation; VOSP – Visual Object and Space Perception; CORVIST – Cortical Vision Screening Test.; N correct – number of items correct.

		Posterior cortical atrophy		**Typical Alzheimer's disease**		
Domain	Test	Mean (SD) [min - max]	Missing data %	Mean (SD) [min - max]	Missing data %	Sig.
Visuoperceptual	Usual views	63.5 (30.8) [0.0 - 100.0]	22.6	91.8 (10.4) [65.0 - 100.0]	13.8	* p < .001
	Unusual views	21.7 (23.6) [0.0 - 95.0]	22.6	55.4 (25.5) [5.0 - 95.0]	13.8	p < .001
	VOSP object decision	54.3 (22.1) [25.0 - 100.0]	0.0	81.6 (11.8) [55.0 - 100.0]	1.7	* p < .001
	VOSP fragmented letters	26.3 (27.8) [0.0 - 100.0]	11.8	71.1 (30.6) [0.0 - 100.0]	3.4	p < .001
Early visual	CORVIST hue discrimination	69.1 (32.7) [0.0 - 100.0]	8.6	81.8 (25.2) [0.0 - 100.0]	5.2	* p = .011
	Crowding (time)	80.2 (21.7) [0.0 – 95.3]	26.9	85.1 (13.4) [0.0 – 93.0]	10.3	* p = .127
	VOSP figure/ground	81.3 (15.2) [50.0 - 100.0]	4.3	91.8 (8.2) [70.0 - 100.0]	3.4	* p < .001
	Efron shape discrimination	74.2 (17.1) [50.0 - 100.0]	4.3	88.6 (15.3) [50.0 - 100.0]	5.2	p < .001
Episodic memory	Recognition (words)	74.4 (16.8) [48.0 - 100.0]	29.0	74.9 (18.8) [48.0 - 100.0]	36.2	p = .891
	Recognition (faces)	81.9 (13.1) [48.0 - 100.0]	1.1	64.2 (13.3) [48.0 - 100.0]	34.5	p < .001
Language	Graded difficulty naming	70.5 (27.5) [0.0 - 100.0]	0.0	64.4 (29.6) [0.0 - 100.0]	0.0	p = .197
	Concrete synonyms	82.1 (15.7) [0.0 - 100.0]	11.8	82.7 (12.4) [48.0 - 100.0]	15.5	p = .821
	Baxter spelling	51.7 (31.9) [0.0 - 100.0]	6.5	58.5 (29.7) [0.0 - 100.0]	10.3	p = .219
Executive/ calculation	Graded difficulty arithmetic	45.3 (18.3) [0.0 - 88.5]	9.7	54.0 (19.3) [0.0 - 88.5]	44.8	p = .027
	Digit span (forwards)	55.5 (21.3) [8.3 - 100.0]	23.7	52.7 (17.4) [16.7 - 100.0]	3.4	p = .411
	Digit span (backwards)	28.3 (14.9) [0.0 - 100.0]	24.7	33.0 (19.9) [0.0 - 100.0]	1.7	* p = .130
	Cognitive estimates	35.2 (22.4) [0.0 - 90.0]	4.3	34.8 (20.8) [0.0 - 90.0]	3.4	p = .910
Visuospatial	Cancellation (N correct)	76.8 (25.7) [0.0 - 100.0]	3.2	95.6 (7.4) [68.4 - 100.0]	5.2	* p < .001
	Cancellation (time)	63.9 (13.9) [0.0 – 89.3]	5.4	52.1 (22.8) [0.0 – 82.2]	5.2	* p = .001
	VOSP number location	30.4 (30.3) [0.0 - 100.0]	4.3	53.5 (40.2) [0.0 - 100.0]	5.2	* p < .001
	VOSP dot count (N correct)	49.2 (33.3) [0.0 - 100.0]	2.2	82.9 (26.3) [0.0 - 100.0]	5.2	* p < .001

	VOSP dot count (time)	74.7 (16.0) [0.0 – 95.7]	49.5	72.2 (18.6) [0.0 – 88.7]	36.2	p = .523

Posterior cortical atrophy

The principal component analysis for the posterior cortical atrophy group was robust (Kaiser-Meyer-Olkin = 0.865) and Bartlett's test of sphericity was significant (approximate $\chi^2 = 1242.972$, d.f. = 231, $p < 0.001$). The 3-factor varimax rotated solution accounted for 61.0% of the total variation in the patients' performance. The variance explained per factor is as follows: Factor 1 (visuoperceptual-early) = 23.0%; Factor 2 (cognitive) = 21.4%; Factor 3 (visuospatial-early) = 16.6%. The factor loadings are shown in Table 3.

Table 3 - Principal components analysis results for posterior cortical atrophy. Factor loadings larger than 0.5 are shaded in grey. Abbreviations: VOSP – Visual Object and Space Perception; CORVIST – Cortical Vision Screening Test.; N correct – number of items correct.

Domain	Test	Factor 1 (visuoperceptual-early)	Factor 2 (cognitive)	Factor 3 (visuospatial-early)
Visuo-perceptual	Usual views	0.894	0.070	0.244
	Unusual views	0.871	-0.037	-0.021
	VOSP object decision	0.857	0.017	0.135
	VOSP fragmented letters	0.648	0.115	0.464
Early visual	CORVIST hue discrimination	0.627	0.198	0.246
	Crowding (time)	0.655	0.222	0.429
	VOSP figure/ground	0.526	0.021	0.460
	Efron shape discrimination	0.454	0.125	0.413
Episodic memory	Recognition (words)	0.770	0.131	0.206
	Recognition (faces)	-0.098	0.548	0.258
Language	Graded Difficulty Naming	0.193	0.781	-0.036
	Concrete synonyms	0.135	0.773	0.103
	Baxter spelling	0.113	0.795	0.165
Executive/ calculation	Graded Difficulty Arithmetic	0.011	0.743	0.342
	Digit span (forwards)	0.128	0.702	0.077
	Digit span (backwards)	-0.052	0.803	0.042
	Cognitive estimates	-0.202	-0.684	-0.225
Visuo-spatial	Cancellation (N correct)	0.365	0.305	0.589
	Cancellation (time)	0.252	0.220	0.542
	VOSP number location	0.237	0.147	0.814
	VOSP dot count (N correct)	0.163	0.037	0.823
	VOSP dot count (time)	0.186	0.318	0.648

Measures that loaded heavily onto the first factor were tests of visuoperceptual function (usual/unusual views, object decision and fragmented letters), early visual processing (crowding, hue discrimination, shape discrimination and figure/ground discrimination), and recognition memory for words. A common feature of these tests is the identification of stimuli based on their perceptual features; hence we called this factor 'visuoperceptual-early'. This component was not significantly correlated with MMSE (r = .094, p = .377), or age (r = -0.201, p = .057).

The second factor comprised high loadings from tests of recognition memory for faces, language abilities (synonym judgement, naming, spelling), and attention/executive tasks (digit span forwards and backwards, arithmetic, and cognitive estimates). This component was significantly correlated with MMSE (r = 0.603, p < .001) and age (r = .334, p = .001). Given the nature of the test loadings and the correlation with MMSE, we termed this factor 'cognitive'.

The final factor was associated with tests of visuospatial processing (dot counting and number location) and letter cancellation. Moderate loadings were also found for tests of early visual processing and identifying fragmented letters. This component had a significant correlation with MMSE (r = 0.398, p < .001) but not age (r = .039, p = .712). These tests overall require scanning of the visual field/visual search, and abstraction of visuospatial relationships between stimuli. Furthermore, variance associated with early visuoperceptual aspects of some of these visual tasks was already accounted for by the first factor. Accordingly, we called Factor 3 'visuospatial-early'.

To visualise variation along these dimensions, all PCA-patient factor scores were plotted (blue diamonds in Figure 1A-C). These scatterplots demonstrate various important findings: (i) within the PCA group there were three main dimensions of variation; (ii) for all three dimensions, the patients varied in graded ways – i.e., there was no evidence of clusters implicating mutually-exclusive subtypes of PCA; (iii) the analyses added evidence to previous suggestions that there are both visuospatial and visuoperceptual presentations of PCA (i.e., some patients presented with greater impairment in one aspect of visual processing than the other, as well as many cases with dual visual deficits); (iv) there are concurrent, varying levels of generalised cognitive impairment in PCA (Figure 1B&C), consistent with it being commonly associated with underlying AD.

Phenotypic continua in typical Alzheimer's disease and Posterior Cortical Atrophy

We explored whether PCA and typical AD cases overlapped with each other in their respective multidimensional spaces, by projecting factor scores of one group into the multidimensional space of the other. Figure 1A-C show the typical AD cases (red squares) projected into the PCA-defined space. Results showing projection of PCA cases into the tAD-defined multidimensional space are shown in **Error! Reference source not found.**.

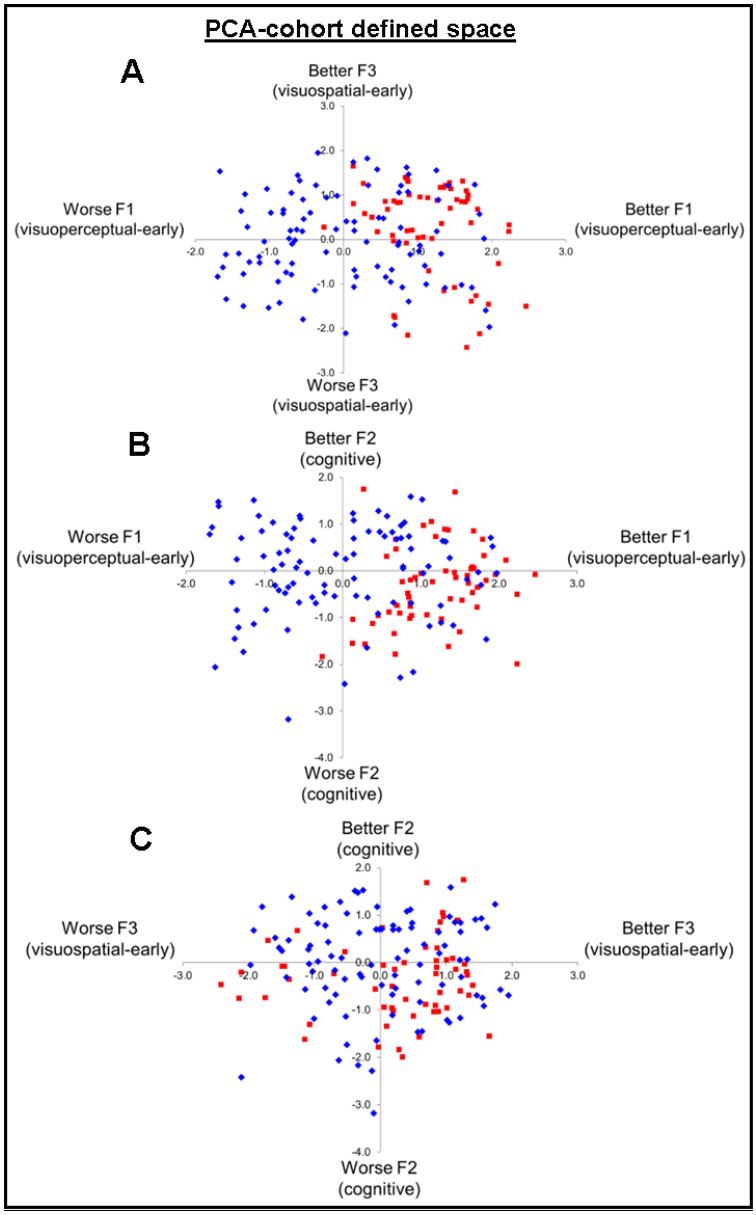

Figure 1 – Graded intergroup phenotypic variation in posterior cortical atrophy and typical Alzheimer's disease. Panels A-C: Typical Alzheimer's disease (tAD) cases projected into posterior cortical atrophy (PCA) multidimensional space. Key: tAD – red squares; PCA - blue diamonds.

These comparative plots illustrate some key observations: (i) there are graded variations along all dimensions in both patient groups; (ii) there is considerable overlap between the tAD and PCA groups on the general cognitive impairment dimension; (iii) the tAD also overlap with the PCA group in terms of the visuospatial and visuoperceptual dimensions (upper-right quadrants of Figure 1A; and the right halves of Figure 1B&C) – again pointing to the observation that the symptomatology of the two groups overlap; (iv) whilst a subset of the PCA cases overlap with the tAD cases, as one would expect, there are PCA cases

with much more pronounced visuospatial and/or visuoperceptual impairment than tAD at the same level of generalised cognitive impairment.

Neural correlates of posterior cortical atrophy multidimensional space

Regional reductions in GM volume in PCA and tAD relative to control groups were consistent with previous investigations (**Error! Reference source not found.**). A detailed summary of the PCA VBM results can be found in Table 4. Lower scores on the visuo-perceptual-early factor (suggesting worse visuo-perceptual function) were associated with decreased right-hemispheric dominant GM volume predominantly in occipital regions. The largest cluster was located in the cuneal cortex and extended inferiorly into the occipital fusiform gyrus and lingual gyrus. Smaller clusters were also found in the occipital pole, lateral occipital cortex, and medial and inferior temporal gyrus. Occipital and occipito-temporal correlates are consistent with the interpretation of this principal component as capturing early visual and visuoperceptual processes.

Lower scores on the cognitive factor were associated with decreased GM volume across a distributed network of left-hemispheric parietal, temporal and frontal regions. The largest cluster within this network was located in the left supramarginal gyrus. The distributed regions associated with performance on this component have been previously associated with higher cognitive functions relating to attention, working memory and phonological processing, implying higher cognitive demands on the tests loading particularly onto this component.

Lower scores on the visuo-spatial-early factor were associated with decreased GM volume predominantly in the right parietal lobe. The largest cluster was located in the right supramarginal gyrus and a smaller cluster located in the superior parietal lobule. These correlates are consistent with the interpretation that this component is capturing variation in spatial and visuomotor processes, both of which place demands on the tests loading particularly onto this component.

Table 4 - VBM results showing brain regions in which GM volume reductions were associated with lower visuoperceptual-early, visuospatial-early and cognitive factor scores in PCA. Rt: right; Lt: left; k: cluster size; P_{FWE}: Family-wise error corrected p-value p<.05 ; x, y ,z: peak-voxel MNI coordinates.

	k	P_{FWE}	T	x	y	z	Brain Region
Visuoperceptual-early	2096	.0001	7.15	14	-75	21	Rt Cuneal Cortex
		.0003	6.58	21	-69	-4	Rt Occipital Fusiform Gyrus
		.0006	6.38	9	-76	0	Rt Lingual Gyrus
	109	.0006	6.40	-12	-42	-39	Rt Occipital Pole
		.0135	5.46	16	-78	-32	Rt Occipital Pole
	24	.0031	5.91	15	-40	-40	Rt Inferior Temporal Gyrus
	81	.0201	5.31	27	-44	-34	Rt Medial Temporal Gyrus
	12	.0231	5.27	-27	-46	-33	Rt Occipital Fusiform Gyrus
	4	.0256	5.23	-20	-39	-33	Rt Lateral Occipital Cortex
Visuospatial-early	124	.0068	5.77	40	-36	34	Rt Supramarginal Gyrus
	69	.0095	5.67	32	-52	44	Rt Superior Parietal Lobule
Cognitive	32	.0092	5.53	-42	-45	38	Lt Supramarginal Gyrus
	21	.0250	5.18	-42	-48	-15	Lt Inferior Temporal Gyrus
	15	.0187	5.28	-56	-44	22	Lt Supramarginal Gyrus
	15	.0200	5.26	-57	-12	-15	Lt Middle Temporal Gyrus
	14	.0107	5.46	-48	4	21	Lt Precentral Gyrus
	14	.0217	5.23	-44	-30	14	Lt Parietal Operculum
	6	.0226	5.21	-48	-40	33	Lt Supramarginal Gyrus
	4	.0215	5.23	-6	-69	44	Lt Precuneus
	2	.0285	5.13	-46	-44	-9	Lt Inferior Temporal Gyrus
	1	.0309	5.02	-36	-9	6	Lt Insula Cortex
	1	.0437	4.97	-62	-27	21	Lt Parietal Operculum

Shared neural correlates of cognition across phenotypes

Overall, plotting tAD within the PCA-defined principal component analysis multidimensional space shows overlapping visual and cognitive profiles. To explore this further, these multidimensional profiles were related to underlying neuroanatomy using whole-brain VBM analysis incorporating a subset of tAD participants with available MRI. Figure 2 shows the results of this combined analysis including patients with PCA and tAD.

In line with the combined analysis comprising mostly PCA participant scans (PCA n=63; tAD n=9), associations between factors and regional GM volume are broadly consistent with analyses restricted to the PCA group. For the largest cluster associated with each principal component, the GM volume in the cluster is plotted against the factor score for every patient in Figure 2Bi-iii. In relation to the distribution of PCA factor scores, the tAD participants appear to be shifted leftwards on cognitive compared to visuospatial-early and visuoperceptual-early factors. At the individual level, several tAD participants exhibit scores on visuoperceptual-early factors and lingual gyral atrophy which are commensurate with PCA group mean scores/atrophy.

Additional correlates identified through combined analysis include lower visuospatial-early factor scores being associated with precuneal GM decreases (Table 5). These may relate to neuropsychological deficits and atrophy patterns (for example, diminished visuospatial functioning and precuneal atrophy) which are common across PCA and tAD, particularly given the relatively young age of our tAD sample.

Table 5 - VBM results showing PCA/tAD shared brain regions in which GM volume reductions were associated with lower visuo-perceptual, visuo-spatial and cognitive factor scores. Rt: right; Lt: left; k: cluster size; PFWE: Family-wise error corrected p-value p<.05 ; x, y ,z: peak-voxel MNI coordinates.

	k	P_{FWE}	T	x	y	z	Brain Region
Visuoperceptual-early	2038	.0003	6.66	8	-75	-2	Rt Lingual Gyrus
		.0003	6.64	10	-74	20	Rt Intracalcarine Cortex
		.0003	6.48	11	-69	-4	Rt Occipital Fusiform Gyrus
	27	.0014	5.99	42	-93	20	Rt Occipital Pole
	26	.0050	5.64	51	-80	8	Rt Lateral Occipital Cortex
	10	.0109	5.42	45	-15	-34	Rt Inferior Temporal Gyrus
	58	.0169	5.26	36	-46	6	Rt Medial Temporal Gyrus
	2	.0446	4.92	-20	-70	-8	Rt Occipital Fusiform Gyrus
Visuospatial-early	120	.0035	5.78	40	-36	34	Rt Supramarginal Gyrus
	44	.0020	6.02	50	-62	24	Rt Lateral Occipital Cortex
	28	.0140	5.28	30	-54	44	Rt Superior parietal lobule
	21	.0186	5.18	46	-28	30	Rt Parietal Operculum
	17	.0139	5.28	6	-46	50	Rt Precuneus
	14	.0240	5.10	30	-44	44	Rt Superior Parietal Lobule
	4	.0385	4.94	4	-51	34	Rt Cingulate Gyrus
Cognitive	69	.0051	5.56	-46	-42	33	Lt Supramarginal Gyrus
	60	.0067	5.46	-42	-48	38	Lt Angular Gyrus
	60	.0107	5.30	-56	-57	-2	Lt Medial Temporal Gyrus
	55	.0411	4.85	-45	-46	18	Lt Inferior Temporal Gyrus
	24	.0143	5.20	-39	-70	-28	Lt Lateral Occipital Cortex
	4	.0211	5.08	-4	-69	44	Lt Precuneus
	4	.0326	4.92	-54	-45	24	Lt Supramarginal Gyrus

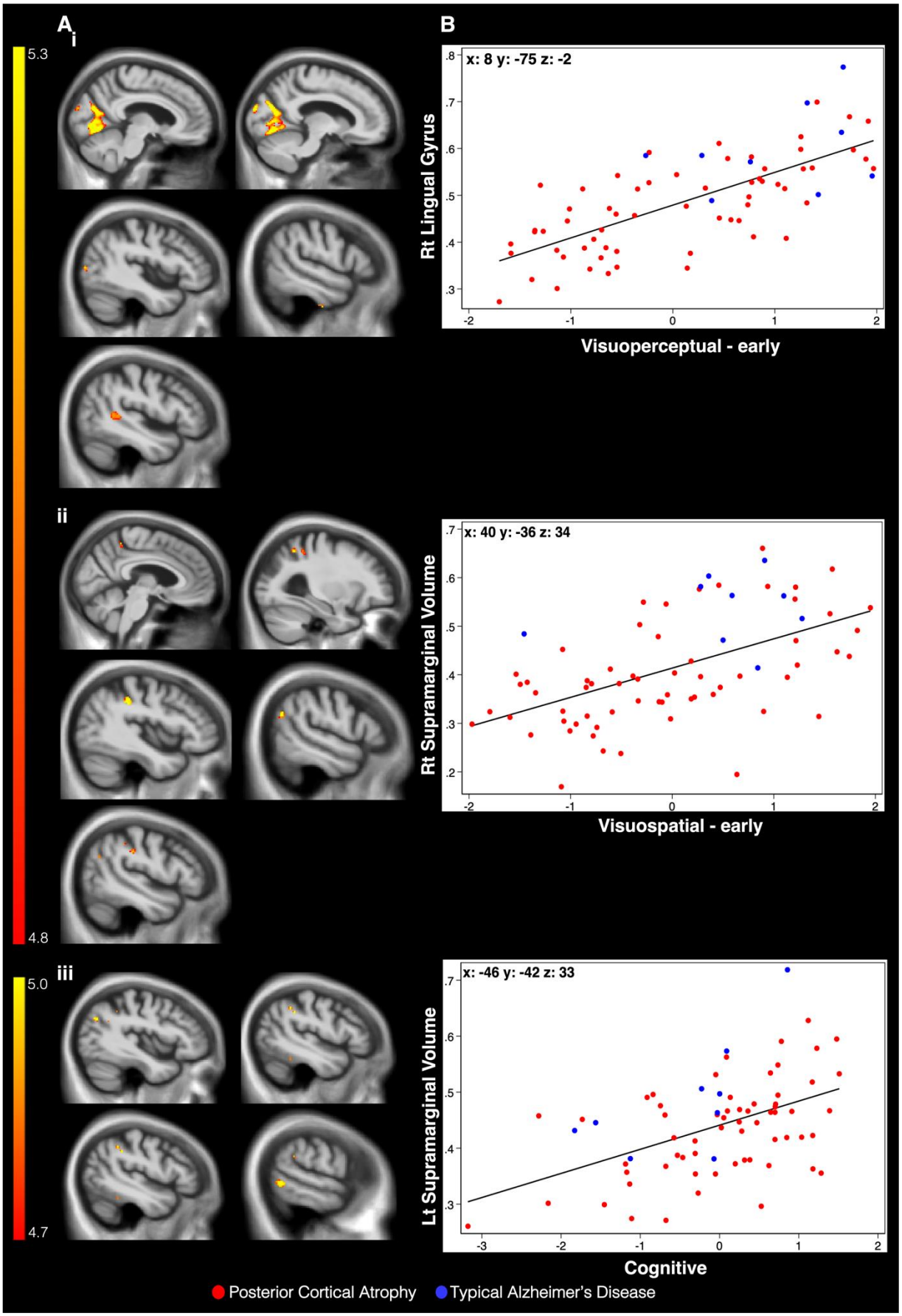
A
i
5.3
4.8
ii
iii
5.0
4.7
B
x: 8 y: -75 z: -2
Rt Lingual Gyrus
Visuoperceptual - early
x: 40 y: -36 z: 34
Rt Supramarginal Volume
Visuospatial - early
x: -46 y: -42 z: 33
Lt Supramarginal Volume
Cognitive
Posterior Cortical Atrophy
Typical Alzheimer's Disease

Figure 2 - Whole-Brain VBM Results in PCA & tAD. Presented are A) statistical parametric maps of significant positive associations between neuropsychological performance and GM volumes in PCA and tAD. FWE-corrected significant p < .05 regions, identified by permutation-based peak-voxel inference, are shown overlaid on normalised study-specific T1-weighted group templates. Colour bar represents t-values.; and B) correlations between neuropsychological scores and participant-specific mean cluster GM volume values (largest significant cluster) by group as scatterplots. MNI coordinates (mm) at peak voxel are shown in bold. Rt: right; Lt: left; i: visuoperceptual-early factor, ii: visuospatial-early factor and iii: cognitive factor.

Discussion

The presence of AD phenotypic variations poses particular challenges for correct diagnosis and clinical management [4, 7]. This large-scale data-driven comparison of PCA and tAD allowed us to consider to what extent varying presentations of AD are separable, mutually exclusive clinical categories or gradedly-different positions within a single, transdiagnostic multidimensional space. We subsequently explored whether the cognitive impairments demonstrated in PCA and tAD were associated with the same neural correlates (or could be driven by atrophy in disparate brain regions). The current study provides evidence of overlapping features (visual, cognitive, and posterior cortical) in a large sample of PCA and tAD participants administered the same detailed neuropsychological battery. These novel comparisons extend work investigating variation within PCA [58, 59] and AD [60], separately.

The results were broadly consistent with the conceptualisation of tAD and PCA as varying continuously on a spectrum of cognitive-neuroanatomical changes: (1) both tAD and PCA data generated dimensions of graded and not clustered variation in terms of generalised cognitive and visual impairments; (2) there was considerable overlap of the two patient groups along these dimensions, (3) the relationship between cognitive impairments and underlying regions of brain atrophy in PCA persisted in tAD. In the remainder of the Discussion, we will consider the graded nature of the identified phenotypic variations and the implications for future clinical research and practice.

Continua of visual processing impairment and cognitive status

Plotting PCA and tAD in the respective multidimensional space from the principal component analysis demonstrated graded variation within and between these groups with respect to visual processing impairments. As expected, a good proportion of the PCA patients had more severe visuospatial and/or visuoperceptual impairments than the tAD cases. However, there was a subset of tAD cases who overlapped with PCA cases on the visual processing dimensions (Figure 1C), indicating visual deficits commensurate with mild to moderate PCA. This finding aligns with previous early reports of AD cases with pronounced visual processing deficits [2, 18] and recent findings suggesting a substantial proportion of tAD patients exhibit predominant visuospatial deficits [61]. Although visual processing impairments are not necessary or sufficient for diagnosis of typical AD, it is generally recognised that visuospatial deficits can be present or emerge later [62]. The profile of tAD with visual deficits commensurate with mild to

moderate PCA was not confined to tAD cases with globally poor performance; some tAD cases presented with impaired visual processing even when their general cognitive status was better than most other cases (top left quadrants of Figure 1C). Overall, these findings provide support for the core hypothesis for this PCA and tAD comparison study, namely that both within and between presentations of AD and PCA, there is evidence of graded variation along phenotypic continua. Specifically, there is evidence of a graded dimension of visual impairment that is independent of variation in general cognitive status.

In addition to the overlap in visual processing impairments, considerable overlap of tAD and PCA on the emergent cognitive dimensions reiterates the importance of non-visual impairments in PCA [6, 63, 64]. Fully characterising cognitive impairments in PCA is important because these symptoms could contribute to the misdiagnosis of PCA [7, 25, 65]. Additionally, highlighting the extent of overlap in cognitive symptoms between typical AD and PCA (and other phenotypes associated with AD) could inform development of treatments and therapies which could be extended to and from typical and atypical AD [66, 67].

Shared neurodegenerative origins of cognitive impairments

The results of the combined VBM analysis suggest that atrophy in the extracted clusters is associated with impairment along the extracted cognitive dimensions, regardless of diagnostic group. Neuroimaging findings imply that overlapping cognitive features in these forms of dementia may arise from atrophy in similar brain regions. This supports the conceptualisation of PCA and tAD as being within a shared, multidimensional phenotypic space, perhaps relating to graded neurodegeneration of functional brain networks [19], rather than as discrete subtypes caused by Alzheimer's disease pathology (for a parallel proposal for the overlapping variations of logopenic progressive aphasia and tAD, see: Ramanan *et al.* [34]).

Implications of graded variation

Our results indicate that a simple categorical distinction between tAD and PCA based on diagnostic criteria would fail to capture the evident graded differences between these phenotypes. This raises the issue of how to relate graded, multidimensional approaches to traditional, categorical classification systems [33, 68]. The latter provide a useful diagnostic short-hand for clinicians, and may be useful for contrastive group-level analysis [69]. We are not proposing that the diagnostic labels should be abandoned entirely. Rather, being able to place cases from different diagnostic categories into a shared, transdiagnostic multidimensional space can highlight key intra- and inter-subgroup variations, enhancing our understanding of the diagnostic categories themselves [29, 30, 33]. This approach is able to capture both graded phenotypic variation, including more atypical examples and mixed cases, as well as highlight more category-like phenotypes if they are present [31]. Thus, a comprehensive 'picture' of an individual

patient could include their broad label and their nuanced multidimensional profile. From a research perspective, this multidimensional approach allows for (and in fact necessitates) a more inclusive recruitment strategy which captures not only the “pure” prototypical cases but the majority of patients, who show graded phenotypic variation. Finally, this approach does not treat potentially central, disorder-related graded variations as sampling noise to be averaged away.

Possible clinical ramifications include identification of: (1) transdiagnostic, potentially treatable symptoms that would otherwise not be evident from research which focusses only prototypical cases; and (2) graded clinico-radiological dimensions also open up the possibility of new approaches to stratification of cases for treatments, dosage titration, and other elements of clinical trials research that are based on scalar rather than categorical variations.

Limitations

Although the cohorts in this study met the respective neuropsychological criteria for tAD and PCA, molecular/pathological evidence of AD was only available for a subset of cases. In future work, it will be important to confirm the molecular/pathological AD status in these cases to extend these findings towards understanding the heterogeneity caused by AD pathology specifically [1]. Principal component analyses, like neuropsychological investigations more generally, are constrained by the types and coverage of the assessments included. The current study was designed to evaluate the characteristic neuropsychological features of PCA along with relatively spared memory, language and executive functions [63, 64, 70]. When new types of assessment are included then additional dimensions can emerge if there is substantive variation of the patient group in this regard [71, 72]. Finally, we note that the tAD group included in this study were relatively young: 15/58 (25%) tAD cases younger than 60. This could mean they were more likely to have a predominant non-memory impairment [14], which could have influenced the overlap in cognitive and visual presentations in our tAD and PCA cohorts. However, it is reasonable to treat these cases as typical AD, because the form of typicality we are referring to here relates to phenotype not age at onset (i.e., young onset AD is not noted as a distinct exemplar of atypical AD in the Dubois *et al.,* [3] criteria), and phenotypic heterogeneity is increasingly recognised in late onset AD too [e.g., 61].

Further applications and future directions

The current study shows that this test-case exploration of phenotypic continua in tAD and PCA has promise for uncovering the nature of variation between different clinical presentations of AD. Future research could extend this beyond tAD and PCA, to explore (i) the full extent of variability in all clinical phenotypes associated with AD pathology, and (ii) variation within PCA due to different aetiologies (e.g., AD, Lewy body disease, corticobasal degeneration [6]). Establishing the underpinning multidimensional

space in these samples would then provide an alternative framework in which variations along each dimension (rather than differences between groups) can be related to the underpinning neuroimaging and neurobiological features [30, 33, 68]. Building from situating tAD and PCA within the same multidimensional symptom-atrophy space, future research could extend this to canonical AD clinical phenotypes to explore the network degeneration hypothesis [1, 7]. This would build on important earlier work [2, 33], which captured graded differences between subgroups of neurodegenerative disease instead of comparing groups of cases based on their diagnostic label.

This multidimensional approach could also inform clinical diagnosis and treatment/management pathways directly. By formally mapping the nature and variation of patients within an aetiology it gives a clearer picture of the patient variations that should be recognised as belonging to each diagnostic group and thus, potentially suitable for tailored interventions. This includes the frequent numbers of patients presenting to diagnostic clinics with a “mixed” clinical syndrome [5], who may in fact represent a coherent position in the graded multidimensional space. Furthermore, establishing the principal components of each aetiology might also generate transdiagnostic treatment options, as has been argued recently for the shared apathy and impulsivity symptomatology observed across different graded subtypes of fronto-temporal lobar degeneration [73].

Acknowledgements

We thank all of the patients, their families, and carers for their continued support of our research programmes. This research was supported by The Rosetrees Trust (A1699), the ERC (GAP: 670428 - BRAIN2MIND_NEUROCOMP), MRC Career Development Award to ADH (MR/V031481/1) and MRC intramural funding (MC_UU_00005/18). The Dementia Research Centre is an Alzheimer's Research UK Co-ordinating Centre and is supported by Alzheimer's Research UK, Brain Research Trust, and The Wolfson Foundation. This work was also supported by the NIHR Queen Square Dementia Biomedical Research Unit and by an Alzheimer's Research UK Senior Research Fellowship [ART-SRF2010-3] and ESRC/NIHR [ES/L001810/1] and EPSRC [EP/M006093/1] grants to SC. KY is an Etherington PCA Senior Research Fellow and is funded by the Alzheimer's Society, grant number 453 (AS-JF-18-003). In memory of Mrs Pam Southerden.

Author contributions

RUI, GP, AH, MALR contributed to the conception and design of the study; KXXY, SC contributed to the acquisition of the data; RUI, DO, GP, AH, DC, MALR, KXXY contributed to the analysis of the data; RUI, DO, GP, AH, DC, MALR, KXXY, SC contributed to drafting the text; RUI, DO, DC, MALR, KXXY contributed to preparing the figures.

Open access

For the purpose of Open Access, the UKRI-funded authors have applied a CC BY public copyright licence to any Author Accepted Manuscript version arising from this submission.

Conflicts of interest

Nothing to report.

References

1. Warren, J.D., P.D. Fletcher, and H.L. Golden, *The paradox of syndromic diversity in Alzheimer disease.* Nature Reviews Neurology, 2012. **8**(8): p. 451.

2. Lambon Ralph, M.A., et al., *Homogeneity and heterogeneity in mild cognitive impairment and Alzheimer's disease: a cross-sectional and longitudinal study of 55 cases.* Brain, 2003. **126**(11): p. 2350-2362.

3. Dubois, B., et al., *Advancing research diagnostic criteria for Alzheimer's disease: the IWG-2 criteria.* The Lancet Neurology, 2014. **13**(6): p. 614-629.

4. Dickerson, B.C., et al., *Approach to atypical Alzheimer's disease and case studies of the major subtypes.* CNS spectrums, 2017. **22**(6): p. 439-449.

5. Koedam, E.L., et al., *Early-versus late-onset Alzheimer's disease: more than age alone.* Journal of Alzheimer's Disease, 2010. **19**(4): p. 1401-1408.

6. Crutch, S.J., et al., *Consensus classification of posterior cortical atrophy.* Alzheimer's & Dementia, 2017.

7. Graff-Radford, J., et al., *New insights into atypical Alzheimer's disease in the era of biomarkers.* The Lancet Neurology, 2021. **20**(3): p. 222-234.

8. Mendez, M.F., M. Ghajarania, and K.M. Perryman, *Posterior cortical atrophy: clinical characteristics and differences compared to Alzheimer's disease.* Dementia and geriatric cognitive disorders, 2002. **14**(1): p. 33-40.

9. Tang-Wai, D.F., et al., *Clinical, genetic, and neuropathologic characteristics of posterior cortical atrophy.* Neurology, 2004. **63**(7): p. 1168-1174.

10. Tang-Wai, D. and M. Mapstone, *What are we seeing? Is posterior cortical atrophy just Alzheimer disease?* Neurology, 2006. **66**(3): p. 300-301.

11. Kaeser, P.-F., J. Ghika, and F.-X. Borruat, *Visual signs and symptoms in patients with the visual variant of Alzheimer disease.* Bmc Ophthalmology, 2015. **15**(1): p. 1-7.

12. Stopford, C.L., et al., *Variability in cognitive presentation of Alzheimer's disease.* Cortex, 2008. **44**(2): p. 185-195.

13. Alves, J., et al., *Posterior cortical atrophy and Alzheimer's disease: a meta-analytic review of neuropsychological and brain morphometry studies.* Brain Imaging and Behavior, 2013. **7**(3): p. 353-361.

14. Migliaccio, R., et al., *Clinical syndromes associated with posterior atrophy early age at onset AD spectrum.* Neurology, 2009. **73**(19): p. 1571-1578.

15. Lehmann, M., et al., *Cortical thickness and voxel-based morphometry in posterior cortical atrophy and typical Alzheimer's disease.* Neurobiology of aging, 2011. **32**(8): p. 1466-1476.

16. Ridgway, G.R., et al., *Early-onset Alzheimer disease clinical variants: multivariate analyses of cortical thickness.* Neurology, 2012. **79**(1): p. 80-84.

17. Crutch, S.J., et al., *The language profile of posterior cortical atrophy.* J Neurol Neurosurg Psychiatry, 2012: p. jnnp-2012-303309.

18. Caine, D. and J.R. Hodges, *Heterogeneity of semantic and visuospatial deficits in early Alzheimer's disease.* Neuropsychology, 2001. **15**(2): p. 155.

19. Seeley, W.W., et al., *Neurodegenerative diseases target large-scale human brain networks.* Neuron, 2009. **62**(1): p. 42-52.

20. Jones, D.T., et al., *Tau, amyloid, and cascading network failure across the Alzheimer's disease spectrum.* Cortex, 2017. **97**: p. 143-159.

21. La Joie, R., et al., *Prospective longitudinal atrophy in Alzheimer's disease correlates with the intensity and topography of baseline tau-PET.* Science translational medicine, 2020. **12**(524): p. eaau5732.

22. Calafate, S., et al., *Synaptic contacts enhance cell-to-cell tau pathology propagation.* Cell reports, 2015. **11**(8): p. 1176-1183.

23. De Calignon, A., et al., *Propagation of tau pathology in a model of early Alzheimer's disease.* Neuron, 2012. **73**(4): p. 685-697.

24. Ahmed, Z., et al., *A novel in vivo model of tau propagation with rapid and progressive neurofibrillary tangle pathology: the pattern of spread is determined by connectivity, not proximity.* Acta neuropathologica, 2014. **127**: p. 667-683.

25. Crutch, S.J., et al., *Posterior cortical atrophy.* The Lancet Neurology, 2012. **11**(2): p. 170-178.

26. Migliaccio, R., et al., *Ventral and dorsal visual streams in posterior cortical atrophy: a DT MRI study.* Neurobiology of aging, 2012. **33**(11): p. 2572-2584.

27. Tsai, P.-H., et al., *Posterior cortical atrophy: evidence for discrete syndromes of early-onset Alzheimer's disease.* American Journal of Alzheimer's Disease & Other Dementias®, 2011. **26**(5): p. 413-418.

28. Lehmann, M., et al., *Basic visual function and cortical thickness patterns in posterior cortical atrophy.* Cerebral cortex, 2011. **21**(9): p. 2122-2132.

29. Butler, R.A., M.A. Lambon Ralph, and A.M. Woollams, *Capturing multidimensionality in stroke aphasia: mapping principal behavioural components to neural structures.* Brain, 2014. **137**(12): p. 3248-3266.

30. Mirman, D., et al., *Neural organization of spoken language revealed by lesion–symptom mapping.* Nature communications, 2015. **6**: p. 6762.

31. Ingram, R.U., et al., *Graded, multidimensional intra-and intergroup variations in primary progressive aphasia and post-stroke aphasia.* Brain, 2020. **143**(10): p. 3121-3135.

32. Ding, J., et al., *A unified neurocognitive model of semantics language social behaviour and face recognition in semantic dementia.* Nature communications, 2020. **11**(1): p. 1-14.

33. Murley, A.G., et al., *Redefining the multidimensional clinical phenotypes of frontotemporal lobar degeneration syndromes.* medRxiv, 2019: p. 19012260.

34. Ramanan, S., et al., *Establishing two principal dimensions of cognitive variation in Logopenic Progressive Aphasia.* Brain Communications, 2020. **2**(2): p. fcaa125.

35. Dubois, B., et al., *Research criteria for the diagnosis of Alzheimer's disease: revising the NINCDS–ADRDA criteria.* The Lancet Neurology, 2007. **6**(8): p. 734-746.

36. Shaw, L.M., et al., *Cerebrospinal fluid biomarker signature in Alzheimer's disease neuroimaging initiative subjects.* Annals of neurology, 2009. **65**(4): p. 403-413.

37. Duits, F.H., et al., *The cerebrospinal fluid "Alzheimer profile": easily said, but what does it mean?* Alzheimer's & Dementia, 2014. **10**(6): p. 713-723. e2.

38. McKhann, G.M., et al., *The diagnosis of dementia due to Alzheimer's disease: Recommendations from the National Institute on Aging-Alzheimer's Association workgroups on diagnostic guidelines for Alzheimer's disease.* Alzheimer's & dementia, 2011. **7**(3): p. 263-269.

39. Dubois, B., et al., *Revising the definition of Alzheimer's disease: a new lexicon.* The Lancet Neurology, 2010. **9**(11): p. 1118-1127.

40. Firth, N.C., et al., *Longitudinal neuroanatomical and cognitive progression of posterior cortical atrophy.* Brain, 2019. **142**(7): p. 2082-2095.

41. Ryan, N.S., et al., *Motor features in posterior cortical atrophy and their imaging correlates.* Neurobiology of aging, 2014. **35**(12): p. 2845-2857.

42. Yong, K.X., et al., *(Con) text-specific effects of visual dysfunction on reading in posterior cortical atrophy.* cortex, 2014. **57**: p. 92-106.

43. Yong, K.X., et al., *Prominent effects and neural correlates of visual crowding in a neurodegenerative disease population.* Brain, 2014. **137**(12): p. 3284-3299.

44. Primativo, S., et al., *The oral spelling profile of posterior cortical atrophy and the nature of the graphemic representation.* Neuropsychologia, 2017. **94**: p. 61-74.

45. Folstein, M.F., S.E. Folstein, and P.R. McHugh, *"Mini-mental state": a practical method for grading the cognitive state of patients for the clinician.* Journal of psychiatric research, 1975. **12**(3): p. 189-198.

46. Willison, J. and E. Warrington, *Cognitive retardation in a patient with preservation of psychomotor speed.* Behavioural neurology, 1992. **5**(2): p. 113-116.

47. Warrington, E.K., *Short Recognition Memory Test for Faces*. 1996: Psychology Press.

48. James, M., G.T. Plant, and E.K. Warrington, *CORVIST: Cortical Vision Screening Test*. 2001: Thames Valley Test Company.

49. Efron, R., *What is perception?*, in *Boston studies in the philosophy of science.*, R.S. Cohen and M.N. Wartofsky, Editors. 1968, D Reidel.: Dordrecht, The Netherlands. p. 137-173.

50. Warrington, E.K. and M. James, *The visual object and space perception battery*. 1991, Bury St Edmunds, UK: Thames Valley Test Company.

51. Ilin, A. and T. Raiko, *Practical approaches to principal component analysis in the presence of missing values.* Journal of Machine Learning Research, 2010. **11**(Jul): p. 1957-2000.

52. Ballabio, D., *A MATLAB toolbox for Principal Component Analysis and unsupervised exploration of data structure.* Chemometrics and Intelligent Laboratory Systems, 2015. **149**: p. 1-9.

53. Ashburner, J. and K.J. Friston, *Unified segmentation.* Neuroimage, 2005. **26**(3): p. 839-851.

54. Nichols, T.E. and A.P. Holmes, *Nonparametric permutation tests for functional neuroimaging: a primer with examples.* Human brain mapping, 2002. **15**(1): p. 1-25.

55. Penny, W.D., et al., *Statistical parametric mapping: the analysis of functional brain images*. 2011: Elsevier.

56. Ridgway, G.R., et al., *Issues with threshold masking in voxel-based morphometry of atrophied brains.* Neuroimage, 2009. **44**(1): p. 99-111.

57. Malone, I.B., et al., *Accurate automatic estimation of total intracranial volume: a nuisance variable with less nuisance.* Neuroimage, 2015. **104**: p. 366-372.

58. Groot, C., et al., *Latent atrophy factors related to phenotypical variants of posterior cortical atrophy.* Neurology, 2020. **95**(12): p. e1672-e1685.

59. Townley, R.A., et al., *Posterior cortical atrophy phenotypic heterogeneity revealed by decoding 18F-FDG-PET.* Brain Communications, 2021. **3**(4): p. fcab182.

60. Jones, D., et al., *A computational model of neurodegeneration in Alzheimer's disease.* Nature communications, 2022. **13**(1): p. 1643.

61. Mukherjee, S., et al., *Genetic data and cognitively defined late-onset Alzheimer's disease subgroups.* Molecular psychiatry, 2020. **25**(11): p. 2942-2951.

62. Kirby, E., S. Bandelow, and E. Hogervorst, *Visual impairment in Alzheimer's disease: a critical review.* Journal of Alzheimer's Disease, 2010. **21**(1): p. 15-34.

63. Hardy, C.J., et al., *Impairments of auditory scene analysis in posterior cortical atrophy.* Brain, 2020. **143**(9): p. 2689-2695.

64. Day, B.L., et al., *Altered visual and haptic verticality perception in posterior cortical atrophy and Alzheimer's disease.* The Journal of Physiology, 2022. **600**(2): p. 373-391.

65. Ahmed, S., et al., *Memory impairment at initial clinical presentation in posterior cortical atrophy.* Journal of Alzheimer's Disease, 2016. **52**(4): p. 1245-1250.

66. Kim, E., et al., *A case with cholinesterase inhibitor responsive asymmetric posterior cortical atrophy.* Clinical neurology and neurosurgery, 2005. **108**(1): p. 97-101.

67. Ridha, B.H., et al., *A double-blind placebo-controlled cross-over clinical trial of DONepezil In Posterior cortical atrophy due to underlying Alzheimer's Disease: DONIPAD study.* Alzheimer's research & therapy, 2018. **10**(1): p. 1-9.

68. Halai, A.D., A.M. Woollams, and M.A. Lambon Ralph, *Using principal component analysis to capture individual differences within a unified neuropsychological model of chronic post-stroke aphasia: revealing the unique neural correlates of speech fluency, phonology and semantics.* Cortex, 2017. **86**: p. 275-289.

69. Zurif, E.B., H. Gardner, and H.H. Brownell, *The case against the case against group studies.* Brain and Cognition, 1989. **10**(2): p. 237-255.

70. Crutch, S.J., et al., *Contributions of patient and citizen researchers to 'Am I the right way up?'Study of balance in posterior cortical atrophy and typical Alzheimer's disease.* Dementia, 2018. **17**(8): p. 1011-1022.

71. Halai, A.D., A.M. Woollams, and M.A. Lambon Ralph, *Investigating the effect of changing parameters when building prediction models for post-stroke aphasia.* Nature Human Behaviour, 2020. **4**(7): p. 725-735.

72. Halai, A.D., A.M. Woollams, and M.A. Lambon Ralph, *Triangulation of language-cognitive impairments, naming errors and their neural bases post-stroke.* NeuroImage: Clinical, 2018. **17**: p. 465-473.

73. Passamonti, L., C. Lansdall, and J. Rowe, *The neuroanatomical and neurochemical basis of apathy and impulsivity in frontotemporal lobar degeneration.* Current opinion in behavioral sciences, 2018. **22**: p. 14-20.